AD NUMBER: AD0861956

LIMITATION CHANGES

TO:

Approved for public release; distribution is unlimited.

FROM:

This document is subject to special export controls and each transmittal to foreign governments or foreign nationals may be made only with prior approval of the Naval Weapons Center, China Lake, CA, 93555; 1 Oct 1969.

AUTHORITY

ST-A USNWC LTR. 30 AUG 1974

NWC TP 4711
COPY 43

CUMULATIVE STRUCTURAL DAMAGE TESTING

by

Thomas B. Cost
Engineering Department

ABSTRACT

Structural degradation of metals due to cyclic loads can be accurately determined if field-incurred damage is correlated with laboratory-induced damage using S/N fatigue gages. Resistance changes can be detected by sensing devices having a resolution between 0.01 and 0.001 ohm. Tests show an average change of S/N gage resistance between 0.096 and 0.116 ohm for field-tested items, where strains were too low to induce detrimental fatigue. Resistance changes between 0.90 ohm at 25,000 cycles to failure and 1.7 ohms at 87,000 cycles to failure were recorded in parallel testing by laboratory-induced cyclic loading. For practical purposes, overtesting and undertesting during cyclic loading of a specimen can be eliminated by use of S/N fatigue gages.

Because fatigue damage is a nonlinear function, resistance changes resulting from a low strain level cannot be extrapolated for higher strain levels. Stringent control over test operation and data acquisition must be exercised to avoid spurious parameters.

Accurate determination of equivalent cumulative damage suggests expanded applications of S/N fatigue gage techniques. Equivalence standards could be developed for random vibration and sinusoidal vibration testing. Correlation of field-incurred damage to cargo with damage induced in the laboratory based on vibration parameters of military specifications should also be developed. Finally, realistic life expectancy and rates for replacement could be determined for items subject to repeated strain loadings, such as helicopter rotors or aircraft arresting hooks.

NAVAL WEAPONS CENTER
CHINA LAKE, CALIFORNIA * OCTOBER 1969

CONTENTS

BLANK PAGE

INTRODUCTION

The Naval Weapons Center (NWC) successfully used S/N fatigue gages (S for strain loading; N for number of cycles to failure) to ascertain structural degradation induced in metallic body structures during transportation tests. Study of this work indicates that a reliable and simple method can be developed to correlate field-induced damage to laboratory controlled equivalent-damage tests by using S/N fatigue gages.

STRUCTURAL DAMAGE MEASUREMENT

This report describes a method used to determine the degree of structural damage incurred by the Chaparral missile during road tests on the XM-370 self-propelled launcher at Aberdeen Proving Ground, Aberdeen, Md. The investigation indicates that field-incurred fatigue damage can be measured using S/N fatigue gages and that field damage can be related to laboratory-induced damage. Because it is not complicated, this method of equivalent-damage testing for measurement of fatigue damage opens a new dimension for product design and evaluation.

THE NATURE OF METALLIC FATIGUE

Microscopic Failure Propagation

Data accumulated using electron microscope and X-ray diffraction techniques support a theory that fatigue damage in metallic structures begins with submicroscopic dislocations or molecular bond lattice slippage of components within a structural member. Fatigue failure (fatigue damage) is generally described as the degradation of a structural member during cyclic stress loading that produces observable strains which are below the yield point. However, the nature of the phenomenon, while recognized and investigated as one mode of structural failure for 100 years, has as yet to be exactly or satisfactorily described.

Fatigue damage is cumulative. Each strain cycle generates some permanent and cumulative strain damage. This is evident from examination of the failure surfaces of completely failed parts, where concentric failure planes start from an initial crack or discontinuity. Microscopic examinations of specimens subjected to repeated cyclic stress loading also display intercrystalline and intracrystalline cracks and dislocations.

Elastic/Plastic Deformation

A general stress/strain curve (Fig. 1) can be divided into a linear (elastic) portion, a nonlinear (plastic) portion, and a transition zone between the two deformation portions. Initially, a specimen to which loading is applied is subject to both elastic and plastic deformation. In the elastic portion

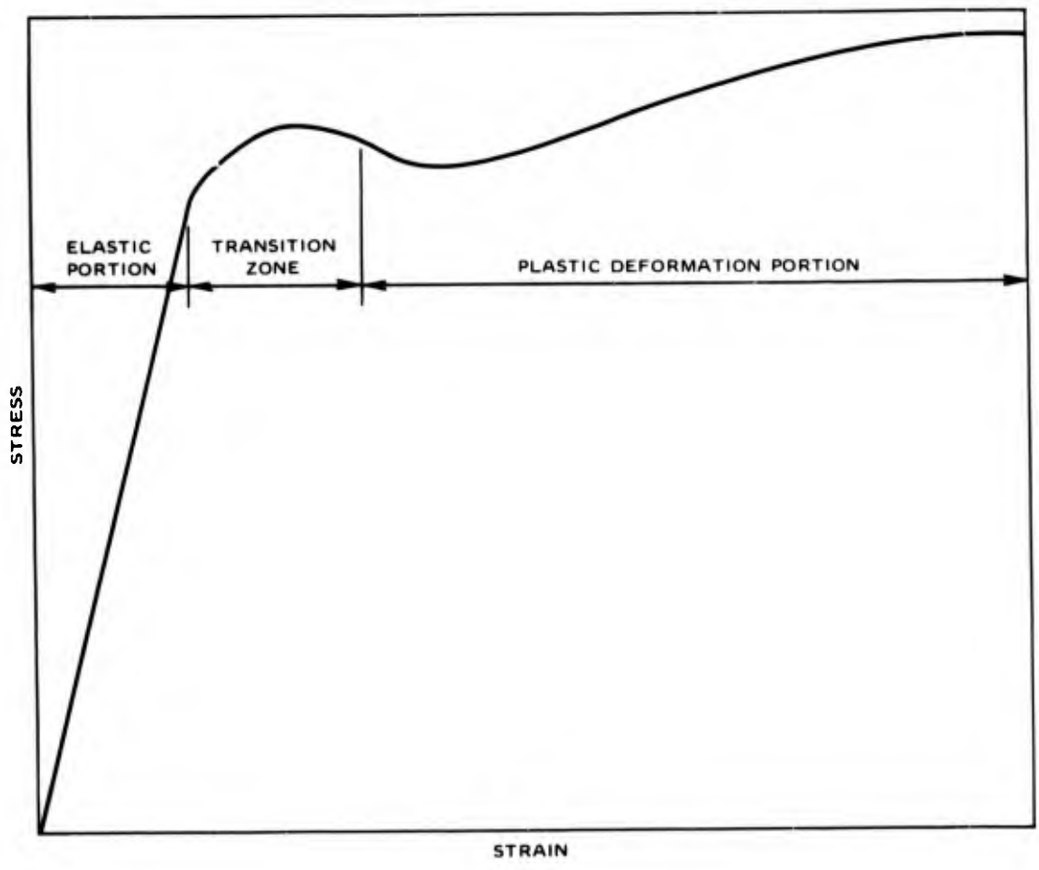

FIG. 1. General Stress/Strain Curve.

of the curve, the component of plastic deformation is very small. The elastic nature of the specimen is predominantly displayed. The magnitude of plastic deformation generally falls within the scatter-band width of the stress/strain curve; this component is normally ignored. As loading is increased, the component of plastic deformation is increased and becomes increasingly important in the transition zone, where, the mode of deformation being undefined, neither plastic nor elastic deformation predominates. In the third portion of the curve, the plastic deformation mode predominates. The elastic mode, while present, becomes insignificant for measurement of overall specimen deformation.

Cyclic Stress Curve Analysis

A hypothetical cyclic stress/strain curve with hysteresis results from strain which occurs in the first portion of the stress/strain curve (Fig. 2). Plastic deformation (strain) is very high relative to the magnitude of the cyclically applied elastic strain. Note that the loop does not close. Each strain cycle causes some damage, and successive applications produce a cumulative, permanent effect. In the transition zone, plastic strain tends to be proportionately greater, relative to applied cyclic strains. As the effect of residual (nonelastic) strain accumulates, dislocation, slippage, or cracking begins on the intra-atomic or the inter-intramolecular level in a confined region and is propagated within or between crystals until, subsequently, macroscopic failure develops.

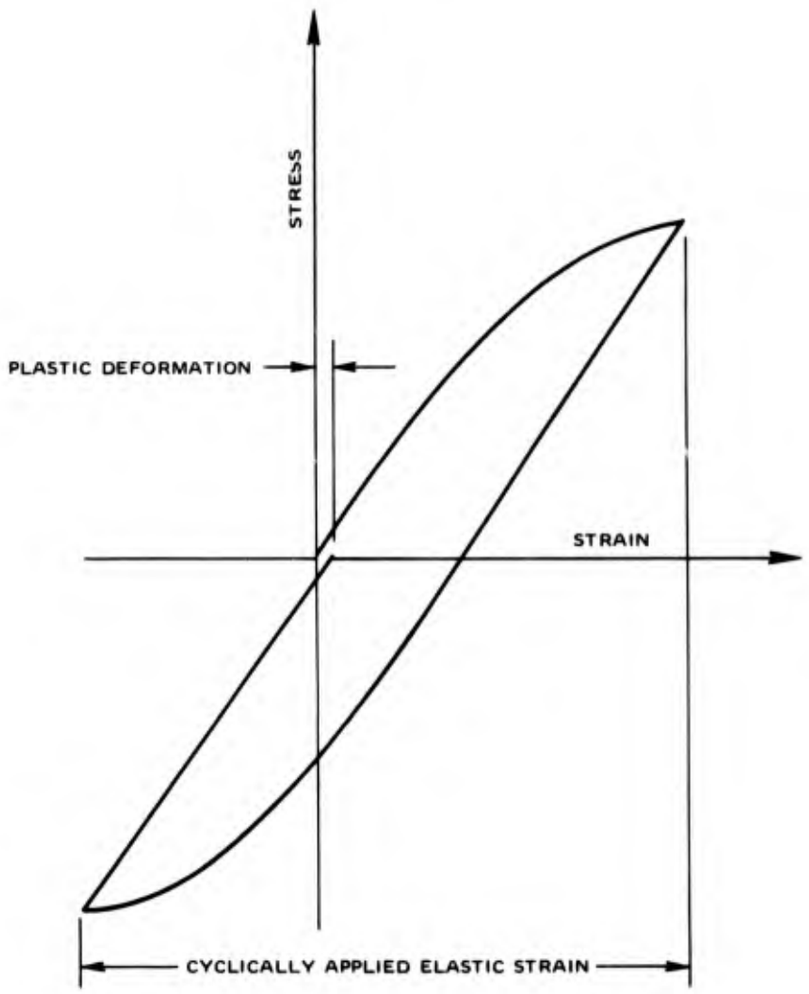

FIG. 2. Cyclic Stress/Strain Curve With Hysteresis.

MEASUREMENT OF FATIGUE PHENOMENA

Statistical Approximation of Fatigue Damage

Parameters affecting fatigue damage include every potential interaction between chemical, physical, mechanical, and metallurgical phenomena which are related to the smelting, heat treating, milling, metal working, fabrication, or use of a specimen. Unpredictable interaction among variable parameters precludes prediction of fatigue failure mechanisms by deterministic methods. Investigation of fatigue phenomena has therefore required a statistical approach. In graphic display of fatigue test data, the number of cycles of applied stress or strain is usually plotted on a logarithmic scale of the abscissa, with some function of the stress or strain level plotted on a linear scale of the ordinate. Stress or strain loading (S) can be plotted against the number of cycles to failure (N) by an approximate least-square fitting of all curve points to broadly scattered data points. Figure 3 shows typical S/N curves.

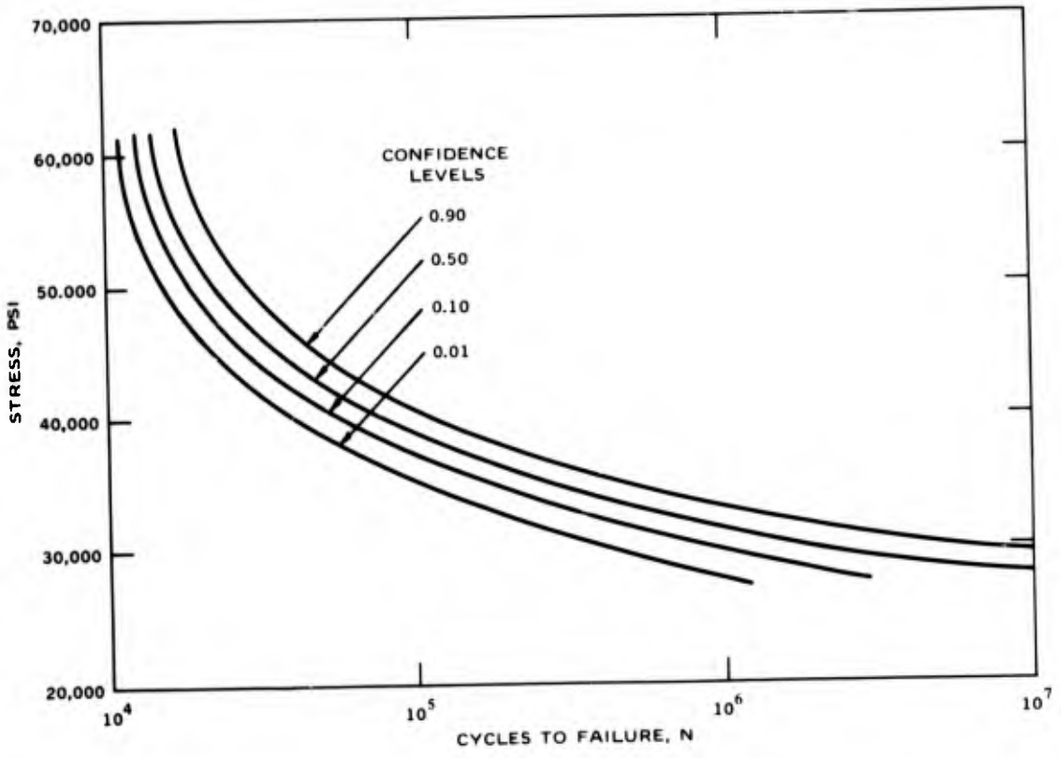

FIG. 3. Typical S/N Curves

Confidence levels in the prediction of failure occurrence can be included only with the collection of considerable data. Such curves are statistical approximations and not absolute predictions of failure, and they are generally applicable to only one material tested under stringent and specific limitations. Unless the complete strain history of a material is known, such curves can provide no insight into a determination of anticipated future life. Sometimes this determination cannot be accomplished even with curves and the strain history. For example, the curves of Fig. 3 cannot be validly applied for a specimen which has been subjected to varying peak strains or to random strain loading.

Treatment of strain data from random loading requires sophisticated equipment and techniques for doing power spectral density and probability density analysis. Complete (or statistically reliable) samples which are representative of the complete strain history are required. Investigation of the power spectral density technique or of the probability density analysis technique are not pertinent here, but are mentioned to illustrate the statistical approach currently required and normally used for the examination of fatigue-failure phenomena. Determination of cumulative fatigue damage before actual failure of a specimen has been largely speculative to date, by reason of random variables and the nonexistence of a testing technique.

Direct Measurement of Fatigue Damage

No effective, uncomplicated, and reliable method of fatigue damage measurement has previously existed that would lend itself to practical application outside a testing laboratory. Fatigue damage

investigation has been done by methods using ultrasonic, eddy-current, or magnetic devices. These devices are often useful for specific purposes, but they are complicated and require sophisticated electronic circuitry. Their use under field conditions would be difficult.

Limited success in fatigue damage measurement has been made through the use of wire-grid or metal-film postyield strain gages. However, these gages, often having shorter fatigue life than the specimens to which they were attached, could not always be adapted to acquire data for the complete test to failure. In 1964 a true S/N fatigue gage was developed by Mr. Darrel R. Harting of Boeing Aircraft Co. (Ref. 1).

The S/N Fatigue Gage

The S/N fatigue gage, unlike a conventional strain gage, does not require continuous monitoring. The gage may be monitored periodically during a test, and resistance changes of the gage can be detected by sensing devices which have a resolution between 0.01 and 0.001 ohm. Figure 4 shows three S/N fatigue gages with different grid, solder-tab, and lead-wire arrangements. Because fatigue damage exhibits a nonlinear function, fatigue gage resistance changes resulting from one particular

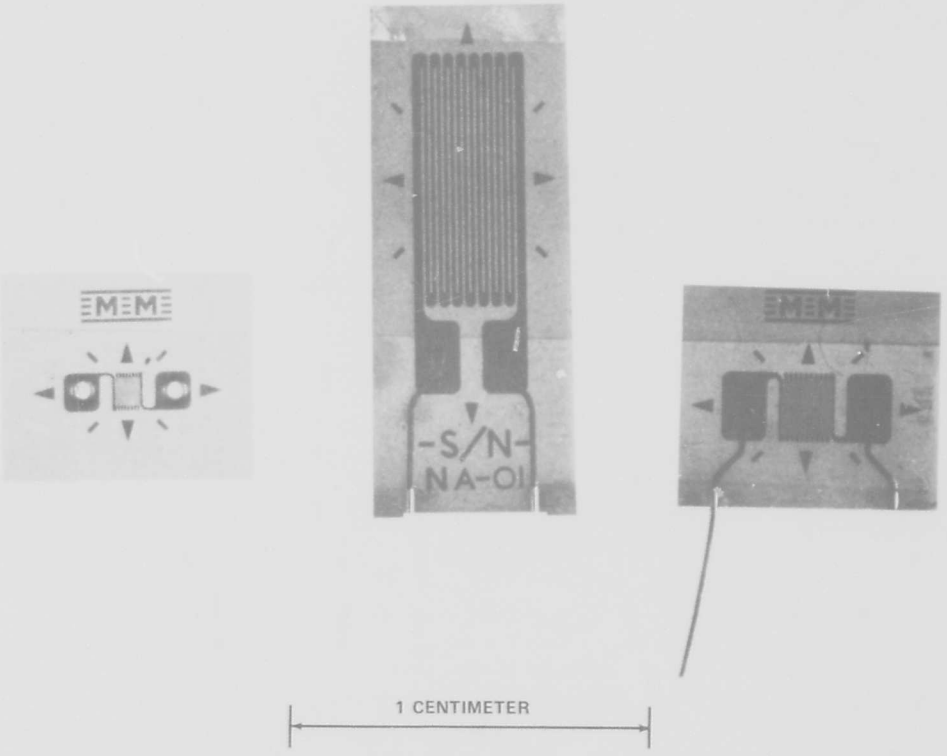

FIG. 4. Typical S/N Fatigue Gages.

strain level cannot be extrapolated for different strain levels. The S/N fatigue gage is fundamentally a strain gage that develops a nonreversible resistance change which is directly correlated to specimen fatigue damage caused by cyclic strains. These resistance changes result from cold-working of the gage grid metal when subjected to cyclic strain. Cold-working of the gage grid produces work hardening (with intracrystalline or intercrystalline dislocation) and causes mechanical interruption of the grid-metal structure, which produces a changed electrical resistance of the gage. Although resistance changes do occur in S/N fatigue gages at strain levels less than 800 μin./in., such changes are very small. The gage appears to "saturate"; that is, it fails to change resistance when subjected to very low strains. As strain levels in the gage increase, however, resistance changes also increase; these can be directly correlated to induced precrack fatigue damage in a specimen. The resistance change for a particular fatigue gage is a function of the strain level environment to which the gage is subjected. Test results with cyclic strain about a zero mean strain were essentially the same as test results with cyclic strain levels above zero mean strain. Fatigue tests using random strain levels produced final resistance changes at failure that were equivalent, within a narrow scatter-band width, to resistance changes at failure from constant peak strain level fatigue tests (Ref. 2).

S/N Gage Location and Mounting

To obtain useful data, the S/N gage, as does a conventional strain gage, requires precise adherence to exacting procedures in locating, orienting, mounting, and installing the gage, and in controlling the test operation and data acquisition. Without previous information on where failure will occur, the strain gradient of a specimen must be determined by the use of brittle lacquer, photoelastic, or other strain measuring techniques to map the strain gradient of the specimen for proper gage location and orientation. The fatigue gage must be aligned with the principal maximum strain and mounted at the point of maximum stress, so that a minimum strain gradient exists across the gage grid. Gage resistance changes from one particular strain level cannot be extrapolated for different strain levels. It is useless to mount a gage on a specimen in an area of low strain with the hope of collecting fatigue data for predicting fatigue damage at higher strain levels by extrapolation. One cycle of strain application at ±3,000 μin./in. causes a gage resistance change 250 times greater than one cycle of strain application at ±1,500 μin./in.

A fatigue gage should be mounted as close as possible to the point of expected failure if it cannot be mounted precisely at that point. Strain sensed by the gage under such conditions must be the highest strain amplitude, relative to the amplitude at the expected point of failure, and must be sufficiently large to cause resistance changes without saturating the gage.

Before the fatigue gage is mounted to a specimen, the surface of the specimen must be smooth, clean, and chemically inert. Two-part epoxy resins normally used for mounting a regular strain gage are recommended for mounting an S/N fatigue gage. Cyanoacrylate adhesives are not recommended for long-term tests or for tests where either high humidity or temperature greater than 150°F are expected. Critical to mounting the gage is the attachment of terminal wires to solder lugs. A gage with factory-installed terminal wires is recommended to lower the possibility of gage damage in the attempt to solder terminal wires after installation. Waterproof coatings are necessary to protect gages from moisture.

Data Acquisition

Extraneous parameters cannot be permitted to bias a test. For test and data acquisition control, the most critical parameter is temperature. Since the S/N fatigue gage is sensitive to temperature change, consecutive resistance readings must be taken at constant temperature, preferably in the range between 75 and 80°F. The gage assumes temporary, temperature-induced strains during temperature fluctuation. These temperature fluctuations are large enough to cause gross errors in data, particularly in the low-cycle portion of a test. Where cyclically applied strain is being introduced to a specimen about a nonzero mean strain, resistance readings must be made with the specimen at the nonzero mean strain and with zero cyclic strain. Great care must be taken to ensure that terminal-wire solder turrets are not damaged and that positive electrical contact is established between probe and turret where lead wires are not used and where a probe from the resistance readout device is placed against a terminal-wire solder turret on the gage. Where pointed-tip probes are used, the solder turret must not be pierced lest the probes be short-circuited on the specimen surface.

CHAPARRAL MISSILE FATIGUE TESTING

The economy, simplicity, and functional flexibility of the S/N fatigue gage made it a logical choice for monitoring fatigue damage on the Chaparral missile while transported on the XM-370 self-propelled launcher.

When the Chaparral missile is mounted on the launcher rails, the warhead, the target detecting device, and the guidance and control section are supported in cantilever-beam fashion ahead of the forward motor tube hanger. The hanger is located immediately aft of the warhead/motor interface station (Fig. 5) and is shown within the circled portion of the inset of Fig. 5. The warhead/motor

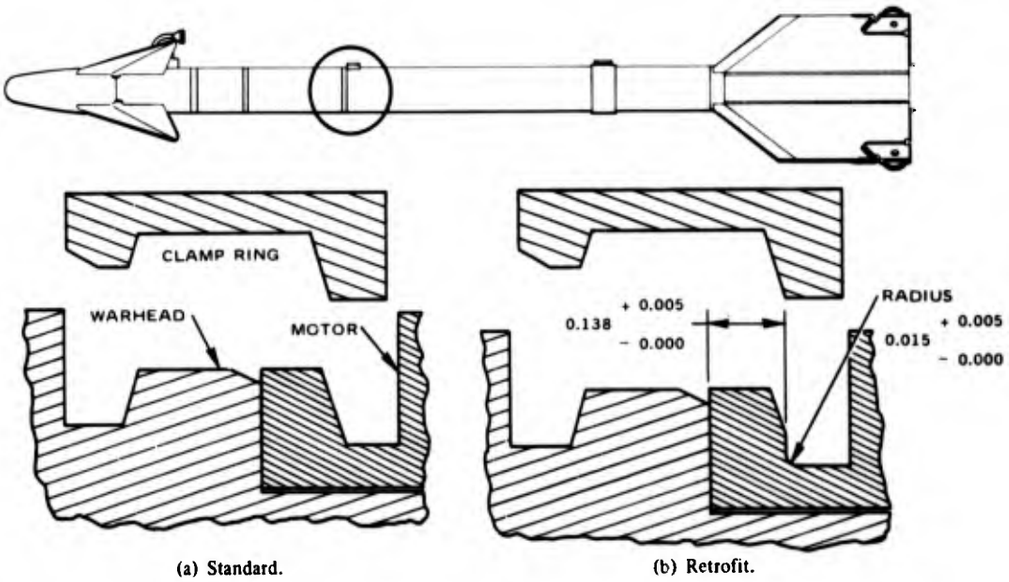

(a) Standard. (b) Retrofit.

FIG. 5. Warhead/Motor Interface Station.

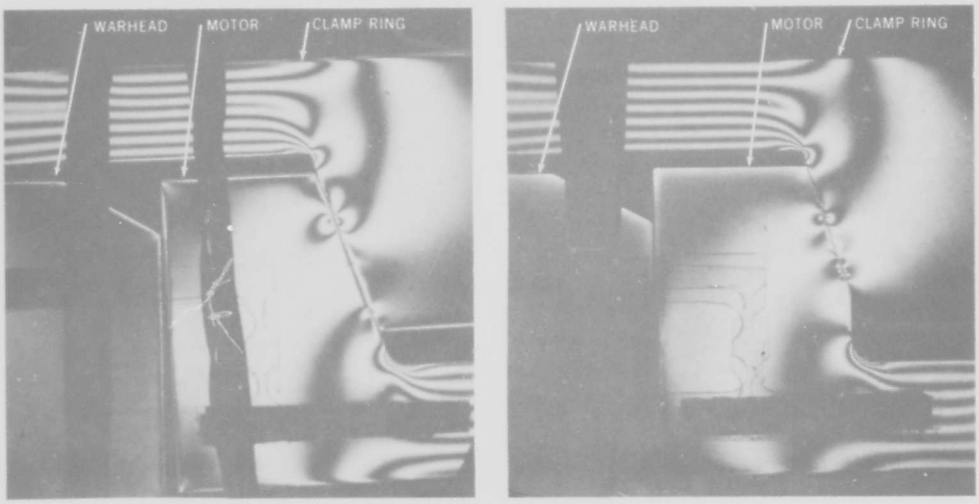

(a) Standard (fringe order 5). (b) Retrofitted (fringe order 4).

FIG. 6. Photoelastic Models of Standard and Retrofitted Motor Tubes Under Strain.

clamp ring grooves are located at the root of this cantilever beam. Theoretical structural analysis of the Chaparral missile (Ref. 3) and data from structural load tests conducted at NWC[1] revealed that if a serious structural problem existed on the missile, the problem would be at the warhead/motor clamp ring grooves, where stress concentrations could possibly exist at the radius on the bottom of the grooves.

The enlargement of the radius at the bottom of the clamp ring grooves (Fig. 5b) was suggested to eliminate the possibility of excessive stress concentration in the motor tube, as exhibited by photoelastic models of standard and retrofitted motor tube configurations (Fig. 6).

When a birefringent material is subjected to strain and examined using interferometric photography, strain acts as a disturbance to one of the two split beams of light. This changes the index of refraction of points within one light beam and causes a shift in the fringes formed on the photographic plate for those regions of full exposure. This fringe shift is proportional to the magnitude of the change; that is, it is proportional to the strain level. The interferometric method permits direct measurement of the difference in local index of refraction.

The standard motor tube configuration has a fringe order of 5 at the radius on the bottom of the groove, whereas the retrofitted tube has a fringe order of 4, with comparatively equivalent strains existing across the bottoms of each groove. This represents a 20% reduction of stress concentration by retrofit design.

[1]Naval Weapons Center. Chaparral Motor Tube/Warhead Interface Structural Testing Report, by T. B. Cost. China Lake, Calif., NWC, 2 July 1968. (Informal memorandum report.)

STATIC LOAD TESTING

Static load tests were conducted on standard and retrofitted motor tubes to determine, by empirical methods, existing strains on the bottoms of clamp ring grooves. Strain gages were mounted on the bottoms of standard and retrofitted motor tube sections. Motor tubes were clamped (one at a time) to an aluminum billet that had been machined to the same dimensions as a warhead. This simulated warhead was then placed in a restraining frame attached to a Baldwin universal testing machine (Fig. 7). At 15 1/2 inches from the warhead/motor interface, static loads were applied in 100-pound increments up to 800 pounds, with a final increment of 60 pounds to produce a maximum shear load of 860 pounds and a moment of 13,330 inch-pounds. This laboratory load application corresponded to the loading generated by a 10-*g* transverse acceleration. Strain values for the standard and retrofitted tubes during these tests were essentially the same. Static loading to failure above 860 pounds produced cracks at the radius on the bottom of the clamp ring grooves in both standard and retrofitted motor tubes.

Vibration tests were conducted on a dummy missile with a standard motor tube to determine missile resonant frequencies. These tests were also used to determine the time to failure for the missile when it was subjected to resonant-dwell tests with a 1-*g* input applied transversely to the longitudinal axis through motor tube hangers. Fatigue gages were mounted in the bottoms of both the warhead and motor tube clamp ring grooves. Several sweeps from 5 to 2,000 cycles were made with a sinusoidal input at ±1 *g*.

Pertinent information gained from vibration tests included these facts:

1. The missile portion which extends (in cantilever-beam fashion) ahead of the front motor hanger has a naturally resonant frequency of 30 cps.

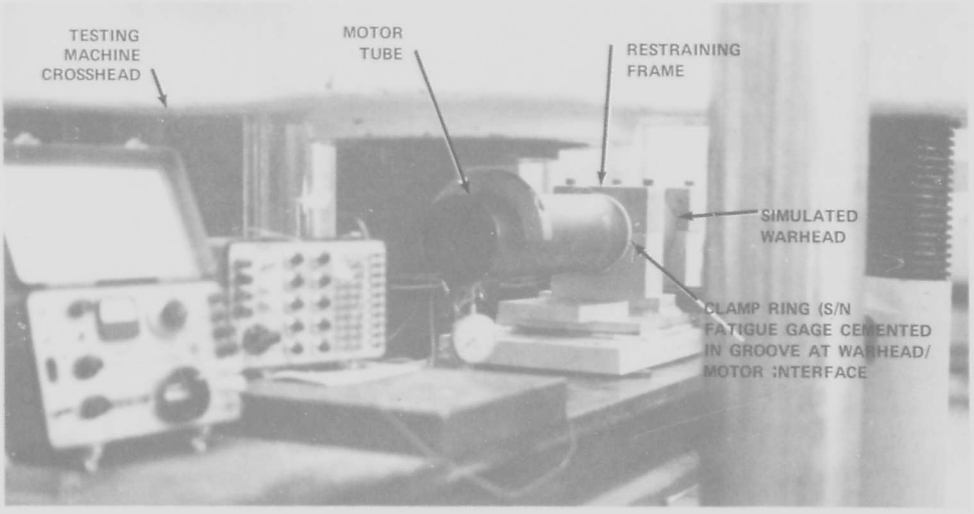

FIG. 7. Static Load Testing Arrangement.

2. An abrupt, catastrophic failure occurred as a peripheral crack in the motor tube at the sharp radius on the bottom of the clamp ring groove after 20 minutes of resonant-dwell vibrations.

3. The resistance change in the fatigue gage on the motor tube was 1.6 ohms, and that in the fatigue gage on the warhead was 0.15 ohm.

MOTOR TUBE GAGE LOCATION

S/N fatigue gages were located on the basis of information gained from dummy missile vibration testing. Even though a fatigue gage could not be mounted on the radius at the bottom of the clamp ring grooves (Fig. 5b), a gage could be mounted in the region immediately adjacent to the radius that would be in a relatively high strain field if one existed at the radius.

The S/N gages so placed would be subjected to fatigue damage commensurate with damage generated in motor tube and warhead clamp ring grooves during the road transportation and cross-country transportation tests. Correlation could then be established between resistance changes incurred during the transportation tests and changes incurred during fatigue tests conducted in the laboratory.

ROAD AND CROSS-COUNTRY TESTING

Twelve Chaparral missiles were instrumented for road and cross-country tests. On each missile, two FNA-06 S/N fatigue gages were mounted on the bottoms of motor tube and warhead clamp ring grooves where the gages would respond to maximum strains in either compression or tension (Fig. 8). The backing on each gage was trimmed as close to the gage grid as possible to aid in mounting the gage immediately adjacent to the sharp radius at the bottom of the grooves.

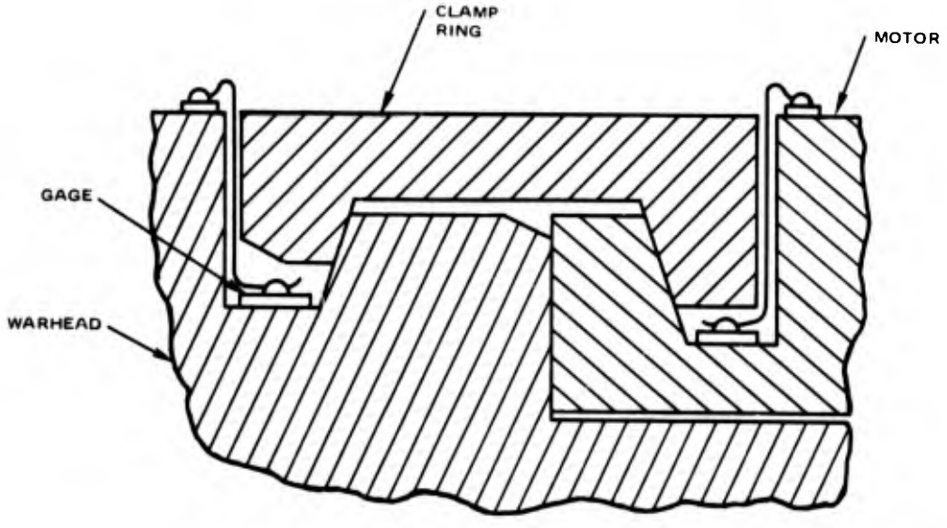

FIG. 8. Locations of S/N Fatigue Gages for Road and Cross-Country Tests.

The missiles were loaded on an XM-370 self-propelled launcher, with four missiles on launcher rails and eight missiles in storage compartments. Missiles were changed from storage rack to launcher rails at periodic intervals during the test to equalize input vibration loadings on each missile. The self-propelled launcher completed 5,000 miles of road transportation and 1,600 miles of cross-country transportation during tests at Aberdeen Proving Ground.

These tests were designed to subject the Chaparral missiles and the self-propelled launcher to worst-case shock and vibration parameters. Upon completion of these strenuous tests, all components were minutely inspected. Dye penetrant and X-ray examinations of the motor tube and warhead clamp ring grooves disclosed no cracks in any of the 12 specimens.

LABORATORY TESTING

Laboratory fatigue tests (to failure) were conducted on five standard motor tube sections and inert warheads and on three modified motor tube sections and inert warheads. A strain gage and an FNA-06 fatigue gage were mounted at the bottom of the clamp ring groove on the warhead of each of these test specimens for data acquisition (Fig. 9). The gages were located on the specimens to respond to maximum induced strain. The warhead/motor specimens were mounted in a restraining bracket and attached by a drive rod and collar to an electrodynamic vibration exciter (Fig. 10). Data acquisition and test monitoring equipment (Fig. 11) consisted of a force gage, signal amplifier, oscilloscope, counter for counting cycles of load application, and resistance-indicating device.

A sinusoidally varying load of ±1,000 pounds peak force was applied to each specimen at 30 cps in a manner that would introduce a moment of 15,000 inch-pounds at the warhead/motor clamp ring grooves. The sinusoidal moment loading, corresponding to loading induced by an 11.6-*g* pulse, developed strain levels of ±1,500 μin./in. on the bottom of the motor tube clamp ring grooves and strain levels of ±100 to ±200 μin./in. in the bottom of the warhead clamp ring grooves.

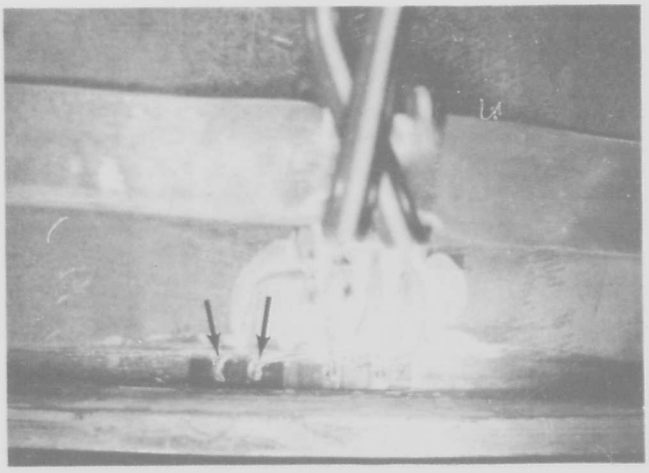

FIG. 9. FNA-06 Fatigue Gage (Left Arrow) and Strain Gage (Right Arrow) Mounted on Chaparral Clamp Ring Groove of Motor Tube for Laboratory Test.

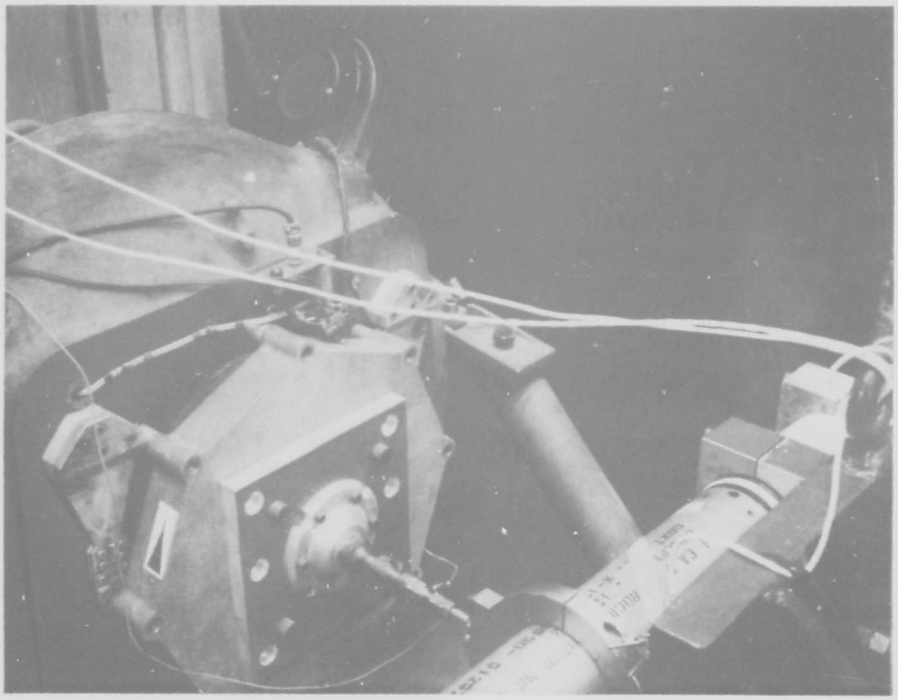

FIG. 10. Vibration Equipment.

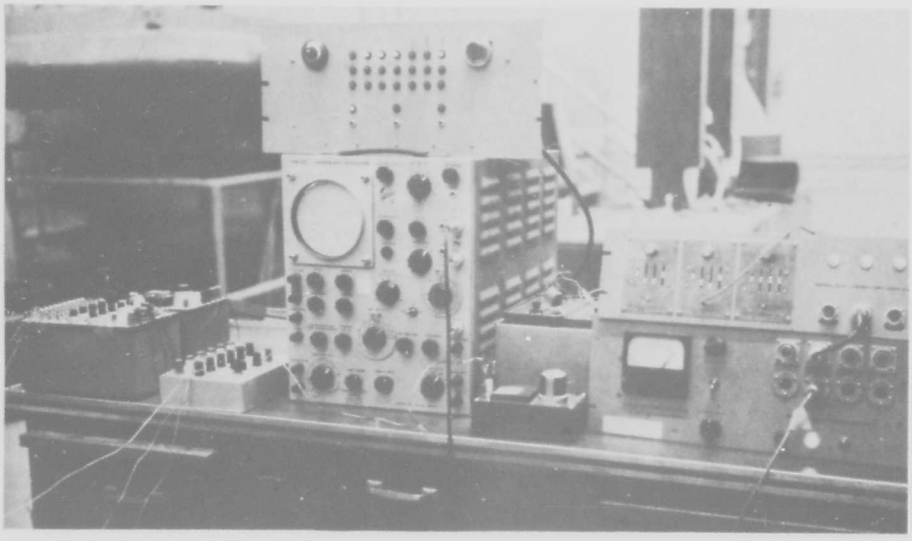

FIG. 11. Data Acquisition and Test Monitoring Equipment.

The tare strains, induced by tightening the clamp ring, were between -70 and +100 μin./in. in the warhead clamp ring grooves and between 185 and 490 μin./in. in the motor tube grooves. Recording of resistance measurements had been planned every 1,000 cycles, up to 10,000 cycles, and every 10,000 elasped cycles thereafter. In two cases, indications for the first 4,000 cycles were not recorded. Loads were applied until failure occurred in the motor tube clamp ring grooves. Parameters were selected on the following concepts:

1. Strain values of ±1,500 μin./in. were above the lower operating limit of the fatigue gages, to make sure that the fatigue gage resistance would increase as cyclic strain increased.

2. Strain at the sharp radius at the bottom of the groove would be much greater than ±1,500 μin./in. Fatigue failure was therefore anticipated in less than 200,000 cycles in standard motor tubes.

3. If an improvement in the stress-concentration factors for the retrofitted motor tubes existed (even though strains on the bottom of the clamp ring groove were the same), improvement would be manifest first by a marked increase in the number of cycles to failure and second by a greater resistance change in fatigue gages on retrofitted motor tubes than on the standard motor tubes because the gage would be subjected to a greater number of strain cycles

4. If the material in the motor tube were sensitive to frequency (possible, but not probable) or if frequency were a fatigue failure parameter, an oscillation of applied strains at 30 cps would correspond to a resonance at 30 cps that produced failure in vibration.

TEST RESULTS

COMPARISON OF ROAD AND LABORATORY TEST RESULTS

Frequency distribution plots of fatigue gage data obtained by the road tests for the warhead/motor joint show resistance changes for gages in both motor tube and warhead grooves (Fig. 12). Resistance changes are of low magnitude. The average change for the motor tube is 0.116 ohm;

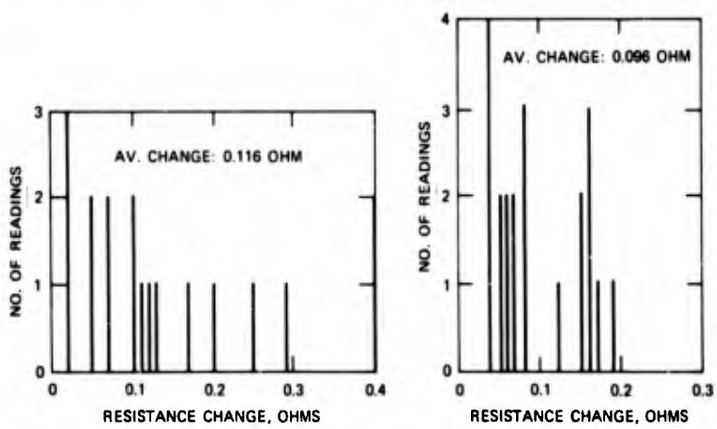

FIG. 12. Frequency Distribution of Fatigue Gage Resistance Changes, Obtained by Road Tests.

the average change for the warhead is 0.096 ohm. Strains of ±100 to ±200 μin./in. for gages on warheads in laboratory tests were too low to induce detrimental fatigue. The gages saturated (that is, stabilized) early in the tests, with resistance changes between 0.04 and 0.20 ohm, which compare favorably with data from road tests and the vibration test.

Data for gages on standard motor tubes (Fig. 13) (resistance change versus cycles to failure) show a spread of resistance changes from 0.90 ohm at 25,000 cycles to failure to 1.7 ohms at 82,000 cycles to failure.

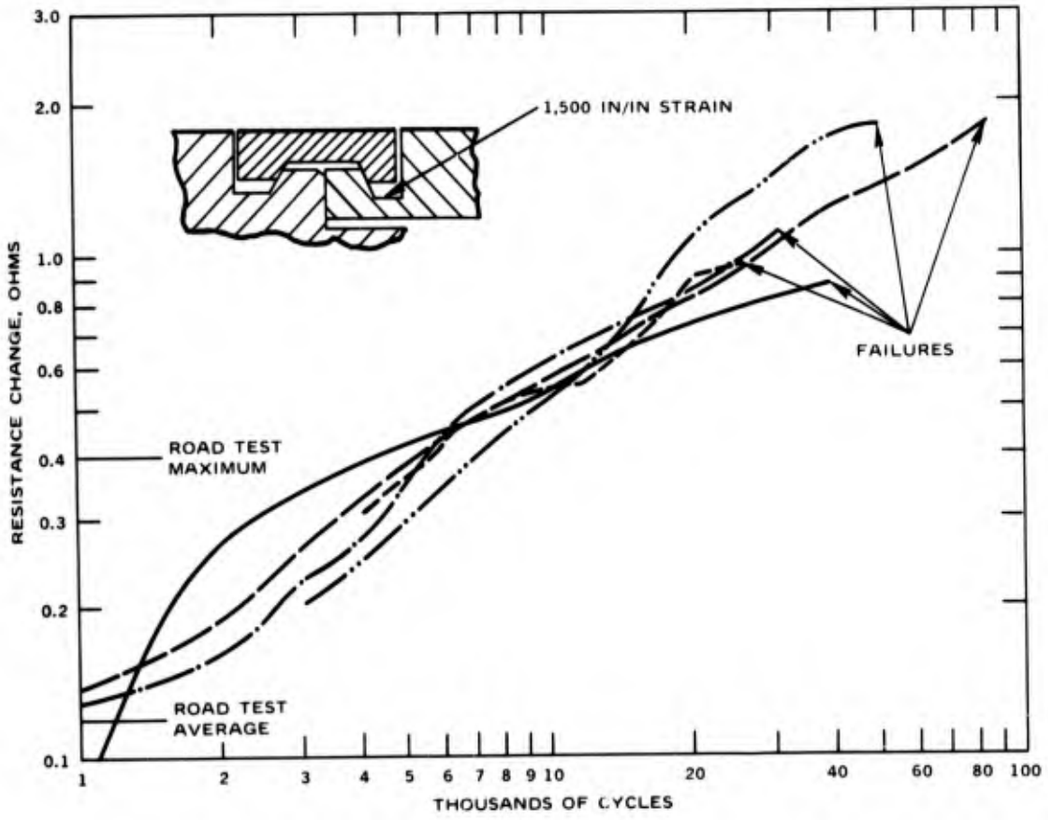

FIG. 13. Fatigue Gage Data for Motor Tubes Subjected to Laboratory Test of 15,000 in-lb Bending Moment at Warhead/Motor Joint. Note comparative road-test data.

LABORATORY FATIGUE TEST FAILURE MECHANISM

Failure detection displayed here is of particular interest, because the two curves with the greatest number of cycles and the greatest resistance changes are for the first two specimens tested. It offers an insight into the failure mode of the specimens. From the abrupt manner in which the motor tube broke during the vibration test (resonant-dwell), fatigue failure produced by the arrangement shown in Fig. 10 was assumed to produce an equally abrupt break. Force gage output and induced dynamic strains were alternately monitored on the oscilloscope to ensure that changes in either force or strain could be detected. During tests on the first two specimens, the force gage output dropped from ±1,000 pounds to between ±950 and ±970 pounds, and the induced strains dropped from ±1,500 to

between ±1,350 and ±1,400 μin./in. and continued to decrease very slowly. Because resistance changes were recorded every 10,000 elapsed cycles, initiation of the first crack failure at the time of the first change of force gage output was not apparent until the rate of resistance increases had changed after two or more consecutive readings. Thereafter, all specimens were checked with dye penetrant at the first sign of force gage output change. Each time, the dye penetrant disclosed a very fine hairline crack at the radius on the bottom of the motor tube groove. Since failures of the first two specimens had not been detected at the moment of first crack initiation, the data show somewhat greater spread than probably existed.

Three modified motor tubes withstood 180,000, 417,000, and 325,000 cycles to failure. Unfortunately, only the first motor (180,000 cycles) had a fatigue gage on it. This gage developed a resistance change of 2.48 ohms. These tests were terminated as soon as the force gage showed a change in output.

CONCLUSIONS

Several conclusions can be drawn from the data:

1. Resistance changes in the fatigue gages on 12 Chaparral missiles used for road and cross-country tests are negligible compared with total resistance changes to failure incurred in the laboratory specimens. The 12 missiles were not structurally degraded during road and cross-country tests.

2. The modification of the motor tubes represents a marked improvement in the fatigue life of the motor tube.

3. The S/N fatigue gage can be used to determine accurately the equivalent structural degradation between field-induced damage and laboratory-induced damage. For all practical purposes, overtesting or undertesting can be eliminated.

4. The proper use of fatigue gages is predicated on the same engineering principles as the use of any other data transducer. Proper installation of gages at correct points on the specimen requires that the stress/strain peculiarities of the specimen be examined by the application of brittle coating, strain gage, or photoelastic techniques, or be assessed through knowledge of previous failures, before instrumentation is begun.

5. Absolute control of the test operation and of data acquisition must be attained to preclude introduction of spurious parameters which compromise test results.

6. To properly define the time of failure, extreme care must be taken to determine the time of first crack initiation.

RECOMMENDATIONS

Applications of this technique should be expanded to

1. Investigate development of equivalence standards in cumulative damage between random and sinusoidal vibration tests.

2. Determine the equivalence between damage to cargo transported by various modes that is field-induced and damage that is laboratory-induced from vibration parameters described in military specifications.

3. Equate controlled-spectrum shock-test damage to classical, shaped, shock-pulse test damage.

4. Determine realistic life expectancy and replacement rates for helicopter rotor blades and housings, aircraft arresting hooks, and other items that are subjected to repeated strain loadings.

REFERENCES

1. Micro-Measurements, Inc. Applications Manual for the -S/N Fatigue Life Gage, 1st ed. Romulus, Mich., Micro-Measurements, August 1966.

2. Society for Experimental Stress Analysis. Proceedings of the Technical Committee on Strain Gages. Westport, Conn. SESA, 16 May 1967.

3. ARINC Research Corp. Worst Case Mechanical Tolerance Analysis of the Warhead Case and Motor Tube Interface for the Chaparral Missile System, by G. Maki and P. Sorensen. Santa Ana, Calif., ARINC, 19 April 1967. (W7-408-TN031-1.)

UNCLASSIFIED

Security Classification

DOCUMENT CONTROL DATA - R & D

(Security classification of title, body of abstract and indexing annotation must be entered when the overall report is classified)

1. ORIGINATING ACTIVITY (Corporate author) Naval Weapons Center China Lake, California 93555	2a. REPORT SECURITY CLASSIFICATION UNCLASSIFIED 2b. GROUP --

3. REPORT TITLE

CUMULATIVE STRUCTURAL DAMAGE TESTING

4. DESCRIPTIVE NOTES (Type of report and inclusive dates)

Final Report

5. AUTHOR(S) (First name, middle initial, last name)

Thomas B. Cost

6. REPORT DATE October 1969	7a. TOTAL NO. OF PAGES 16	7b. NO. OF REFS 3
8a. CONTRACT OR GRANT NO. Army MIPR A-3168-V-49-3230 b. PROJECT NO. c. d.	9a. ORIGINATOR'S REPORT NUMBER(S) NWC TP 4711 9b. OTHER REPORT NO(S) (Any other numbers that may be assigned this report)	

10. DISTRIBUTION STATEMENT

THIS DOCUMENT IS SUBJECT TO SPECIAL EXPORT CONTROLS AND EACH TRANSMITTAL TO FOREIGN GOVERNMENTS OR FOREIGN NATIONALS MAY BE MADE ONLY WITH PRIOR APPROVAL OF THE NAVAL WEAPONS CENTER.

11. SUPPLEMENTARY NOTES	12. SPONSORING MILITARY ACTIVITY U.S. Army Missile Command Redstone, Alabama

13. ABSTRACT

Structural degradation of metals due to cyclic loads can be accurately determined if field-incurred damage is correlated with laboratory-induced damage using S/N fatigue gages. Resistance changes can be detected by sensing devices having a resolution between 0.01 and 0.001 ohm. Tests show an average change of S/N gage resistance between 0.096 and 0.116 ohm for field-tested items, where strains were too low to induce detrimental fatigue. Resistance changes between 0.90 ohm at 25,000 cycles to failure and 1.7 ohms at 87,000 cycles to failure were recorded in parallel testing by laboratory-induced cyclic loading. For practical purposes, overtesting and undertesting during cyclic loading of a specimen can be eliminated by use of S/N fatigue gages.

Because fatigue damage is a nonlinear function, resistance changes resulting from a low strain level cannot be extrapolated for higher strain levels. Stringent control over test operation and data acquisition must be exercised to avoid spurious parameters.

Accurate determination of equivalent cumulative damage suggests expanded applications of S/N fatigue gage techniques. Equivalence standards could be developed for random vibration and sinusoidal vibration testing. Correlation of field-incurred damage to cargo with damage induced in the laboratory based on vibration parameters of military specifications should also be developed. Finally, realistic life expectancy and rates for replacement could be determined for items subject to repeated strain loadings, such as helicopter rotors or aircraft arresting hooks.

DD FORM 1 NOV 68 1473 (PAGE 1)

S/N 0101-807-6801

UNCLASSIFIED

Security Classification

UNCLASSIFIED
Security Classification

14 KEY WORDS	LINK A		LINK B		LINK C	
	ROLE	WT	ROLE	WT	ROLE	WT
Metal-Fatigue Testing Chaparral Missile Fatigue Tests S/N Fatigue Gage						

DD FORM 1 NOV 68 1473 (BACK)
(PAGE 2)

UNCLASSIFIED
Security Classification